ELSEVIER

Sensors and Actuators B 29 (1995) 261–267

SENSORS AND ACTUATORS B CHEMICAL

Waveguide surface plasmon resonance sensors

R.D. Harris, J.S. Wilkinson

Optoelectronics Research Centre and Department of Electronics and Computer Science, University of Southampton, Southampton SO17 1BJ, UK

Abstract

Planar waveguide surface plasmon resonance sensors have great potential for use in the field of environmental monitoring. In this paper we present a rigorous model for the optical power transmittance of this type of sensor. This model is used to determine the change in transmitted power when a thin layer is adsorbed to the metal-clad region of the sensor, as a function of the waveguide and metal film parameters. Design curves for sensors based upon glass waveguides coated with thin gold films immersed in water are presented. Experimentally determined changes in the output power of a waveguide surface plasmon sensor, as a function of the length of the gold film, are presented and compared to theory.

Keywords: Surface plasmon resonance sensors

1. Introduction

The exploitation of the potential of guided-wave optical biosensors for environmental monitoring is becoming more widespread. In particular, planar waveguide technologies offer the possibility of producing compact, monolithic, multisensor devices which may be connected to instrumentation using optical fibres, allowing remote operation. Optical evanescent field-sensing techniques presently under investigation include grating couplers [1], waveguide interferometers [2,3] and surface plasmon resonance (SPR) sensors [4]. In the latter case, the surface plasmon is generally excited using a 'bulk' optical component such as a prism, and equipment using this technique is now commercially available for the laboratory environment [5]. One potential advantage of the SPR technique is that the metal film which supports the surface plasmon may also be used as an electrode for electrochemical control of sensing reactions [6]. Also a gold-coated SPR device provides an alternative surface for immunoassay. However, recent reports have indicated that the 'bulk' SPR devices may not ultimately be as sensitive as fully guided-wave approaches such as the Mach–Zehnder interferometer [7]. An alternative to the 'bulk' SPR devices which has recently emerged is the use of distributed coupling between a dielectric waveguide and the surface plasmon mode in a metal-coated waveguide [8]. This has the advantage of combining greater design flexibility and the potential for monolithic integration, with the well-established technique of SPR. At present no adequate model for the performance of these devices exists.

In this paper we present a rigorous model for the optical power transmittance through waveguide SPR sensors based upon a step-index slab waveguide approximation. The general configuration of the device modelled is detailed in Fig. 1. The performance of such devices requires analysis of the waveguide modes supported by the metal-clad waveguide, of their excitation by an input waveguide and of the resultant power coupled into an output waveguide. The number of modes in the structure and their complex effective indices which yield modal velocity and attenuation are first numerically evaluated using the argument principle method (APM) [9]. The coupling of power from a monomode input waveguide across a step discontinuity into each mode of the metal-clad region is determined using appropriate overlap integrals [10]. The modes are then allowed to propagate over the length of the metal-clad region, incurring losses due to the imaginary parts of their effective indices. Finally, the total power coupled from these modes into the output waveguide is determined to yield the input/output characteristic of the sensor.

The model allows the determination of the modulation in output power of the sensor due to the adsorption of a thin organic layer to the sensor surface, which

SSDI 0925-4005(95)01692-O

in turn leads to a measure of sensitivity. The sensitivity of these devices may be optimized by adjusting the composite waveguide design, and design curves for sensors based upon glass waveguides coated with thin gold films, for use in the aqueous environment, are presented. Practical, sensitive, waveguide surface plasmon sensors for an aqueous environment, optimized for specific sensing films, are predicted.

A vital part of the sensor design process is to validate experimentally the theoretical predictions of device performance created using the model reported here. In Section 4 of this paper we present experimentally determined changes in the output power of a basic planar waveguide SPR sensor as a function of the metal film length and compare the results with theory. The devices were tested using TM and TE modes with air, and subsequently water, as the superstrate material of the metal-clad regions of the structures.

2. Waveguide design tool

The planar SPR waveguide sensor shown in Fig. 1 must be broken down into two parts to be fully analysed by the waveguide design tool. Region (i) is considered to be a lossless single-moded single-layer input and output waveguide. This region of the sensor is solely employed to couple light into and out of the multilayer region of the device. The multilayer metal-clad part of the device forms region (ii) of the sensor

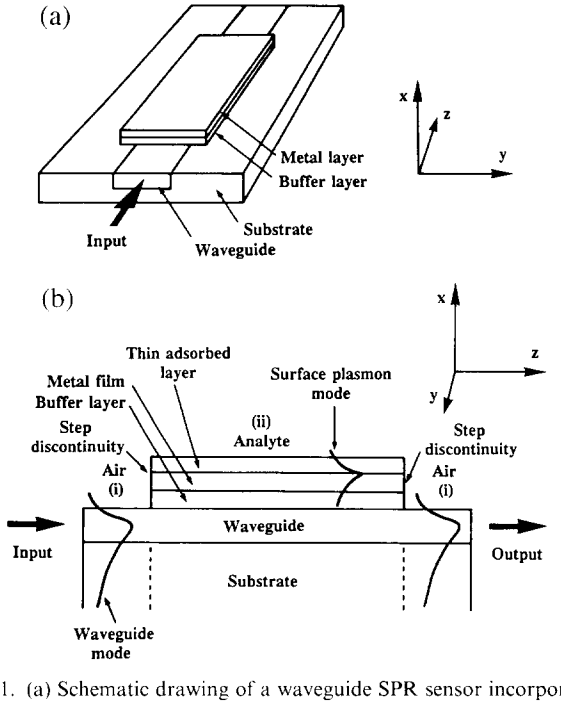

Fig. 1. (a) Schematic drawing of a waveguide SPR sensor incorporating a buffer layer. (b) The lower drawing illustrates the different regions of the sensor and the relevant field profiles.

and acts as the interaction zone with the test sample.

The first step taken in calculating the power transmitted through the sensor is to analyse the modes of the multilayer region of the sensor, region (ii). Absorbing multilayer waveguide structures have been investigated for many years, and devices in which the absorption is provided by the presence of a metal film are of particular interest [11–13]. The theoretical approaches to studying multilayer waveguides are very varied. All of these techniques revolve around the need to form the characteristic eigenvalue equation of the system under consideration [14,15], and then locate the roots of this equation. In order to study general multilayer structures it is necessary to employ a transfer matrix approach [16–18].

The waveguide design tool described here utilizes a system transfer matrix approach to evaluate numerically the eigenvalue equation of a given multilayer waveguide stack. A system transfer matrix characterizes the behaviour of a multilayer waveguide by relating the electromagnetic fields in the substrate of the multilayer region to those in the superstrate [16]. The matrix is formed from the product of each of the layer matrices which define the properties of each individual layer in the waveguide stack. The guidance condition for the waveguide results from the requirement that there is no exponentially growing field in the substrate or the superstrate of the multilayer stack, leading to the characteristic eigenvalue equation [19].

Once the characteristic eigenvalue equation has been determined from the system transfer matrix the waveguide design tool employs the APM to count rigorously and locate the roots to the TE and TM modal eigenvalue equation [9,19]. The APM relates the number of zeros of an analytical function to the contour integral in the complex plane. In this case the analytical function is the eigenvalue equation and the complex plane is that of modal dispersion and absorption. When the number of roots to the eigenvalue equation is known, the waveguide design tool locates them using Müller's complex root finding technique [20].

The waveguide design tool described here does not analyse the leaky modes of a given waveguide system. This is justifiable if the coupling into leaky modes in the multilayer region of the sensor is minimized by using small step discontinuities between regions (i) and (ii) of Fig. 1. Also, light coupling into a leaky mode will, generally, propagate away from the waveguide very rapidly and be lost from the interaction region.

Fig. 2 illustrates the change in loss of a TM mode in the metal-clad multilayer waveguide with the parameters given, as a function of the superstrate index. It serves to indicate how a metal-clad system can be considered as a coupled mode structure. The coupling can be seen to be between a waveguide mode and a surface plasmon mode formed at the interface between

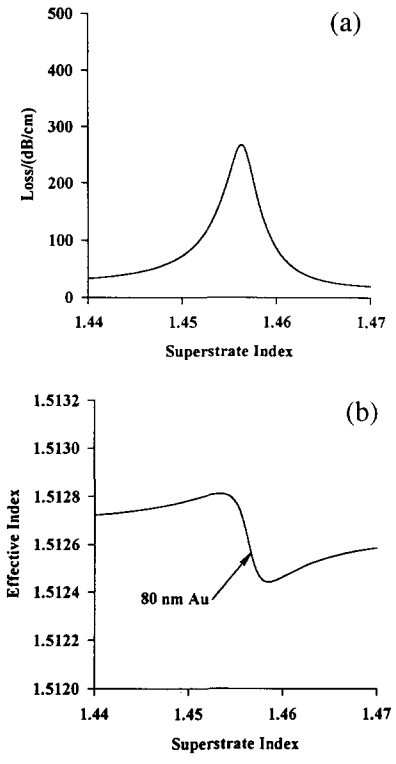

Fig. 2. Variation in (a) loss and (b) effective index of a TM mode in a multilayer gold-coated waveguide, without a buffer layer, as a function of the superstrate index. System parameters: guide index, 1.52; guide depth, 2 μm; substrate index, 1.512; $\lambda = 858$ nm.

the metal and the adjacent dielectric. The losses of the mode peak when it is phase matched to, and hence couples with, the surface plasmon mode. In this instance the electromagnetic fields of the mode are concentrated in the metal film of the device and consequently undergo strong absorption. This situation is accompanied by a perturbation in the real part of the effective index of the mode, analogous to a classical damped oscillator, as also shown in Fig. 2. At this phase-matched point the electromagnetic fields of the mode are almost evenly balanced between the waveguide and the surface of the metal film.

The second step taken in calculating the power transmitted through the structure of Fig. 1 is to analyse the modal coupling between regions (i) and (ii). Here the multilayer part of the sensor, region (ii), is being excited from a monomode input waveguide, resulting in a step discontinuity between the two regions. The output waveguide is then excited across a similar discontinuity. The discontinuity in the waveguide will produce a reflected guided mode and forward and backward travelling radiation modes, as well as the guided mode transmitted in the multilayer structure [21]. Due to the use of small discontinuities in the sensor design the scattering into the forward radiation modes is small and therefore not calculated.

The waveguide design tool evaluates the modal coupling across the waveguide discontinuities in the following manner. The input and output single-layer single-moded waveguides are assumed to be identical and lossless. The required TM, or TE, modal index of this waveguide is located by using the bisection method on the wholly real eigenvalue equation. Once the input mode and the modes in the multilayer region of the sensor have been located the modal expansion coefficients are calculated using the necessary overlap integrals depending on the mode being studied [10]. These overlap integrations are carried out within the waveguide design tool using Simpson's rule.

After determining the expansion coefficients of the modes in the multilayer region of the device these modes are propagated through the length of the metal-clad region of the sensor before being coupled into the output waveguide and the power transmitted through the device calculated. Fig. 3 illustrates the power transmission properties of a planar waveguide SPR sensor, without a buffer layer, as a function of the superstrate index. The output power has been normalized with respect to the input power. The plot is similar to the attenuated total reflection curve observed for a Kretschmann configuration 'bulk' SPR device. The minimum in the power transmission through the device is coincident with the peak modal losses demonstrated by Fig. 2. It is clear that the minimum coincides with phase matching to a surface plasmon mode in the sensor.

The device described here forms the basis of a waveguide SPR sensor. However, designs of sensors are required that will allow device operation in water and some suitable sensor structures are reported in the next section.

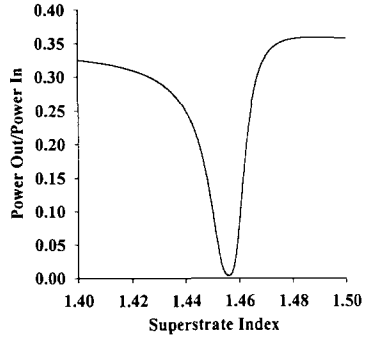

Fig. 3. Plot of normalized output power against superstrate index for a gold-coated multilayer planar waveguide stack, without a buffer layer. System parameters: gold thickness, 80 nm; film length, 2.0 mm; guide index, 1.52; guide depth, 2 μm; substrate index, 1.512; $\lambda = 858$ nm.

3. Design of waveguide SPR sensors

The design process has been carried out with the aim of achieving the greatest change, δP, in the transmitted power through the sensor on adsorbing a thin dielectric film to the surface of the metal layer in the sensor. Designing the sensors for use in an aqueous environment has necessarily been of an iterative nature due to the numerical procedure employed to study the waveguide designs. The problem is compounded by the wide range of device variables that need to be considered and which can be studied using the flexibility of the waveguide design tool.

The establishment of this waveguide design tool has produced a unique opportunity to study the design of waveguide SPR sensors with rigour. While all of the material parameters of an absorbing multilayer waveguide may be altered as a program variable, such a wide range of possibilities is not compatible with practical constraints on material availability. The main material limitations are the substrate material, and subsequent waveguide manufacture, the availability of practical buffer layer materials, the choice of metal for forming the sensor surface and the operating wavelength.

Early investigations into sensor design highlighted that the use of a low index substrate glass allowed for the easiest phase matching between waveguide and surface plasmon modes in a device when operating in water. Using potassium ion exchange to create waveguides in the substrate material offers several clear advantages [22–24]. In particular, it results in waveguides with a low index change. This is very useful for keeping the effective indices of the guided TM modes as close to the substrate index as possible, and allows efficient coupling to optical fibre.

Another method for altering the phase-matching conditions between the surface plasmon and the waveguide modes is to use a low refractive index buffer layer inserted between the waveguide and metal, as shown in Fig. 1. The buffer layer serves the twin purpose of increasing the propagation distance of the surface plasmons [25] and shifting the location of the peak modal losses in terms of the refractive index of the superstrate. Appropriate choice of a buffer layer material allows phase matching to occur in water and may increase the range of the surface plasmons above 1 cm [25]. Some of the most promising materials for use as buffer layers are polymers, which have been made into optical quality films for some years [26]. Early studies involved films with refractive indices in the range 1.486–1.68 and are not particularly useful for waveguide SPR sensors. Recently, polymers have been fashioned as optical quality films with a refractive index of about 1.29. Such a material is an ideal candidate for the buffer layer in a waveguide SPR sensor.

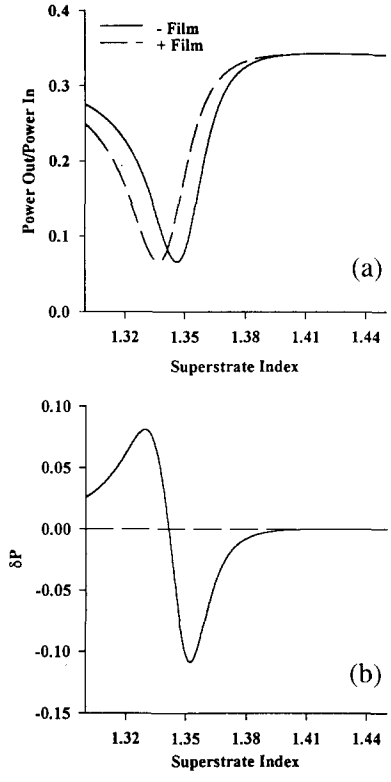

Fig. 4. Performance of a waveguide SPR sensor, without a buffer layer, based on a low refractive index substrate glass and operated at a wavelength of 633 nm: (a) normalized output power and (b) change in normalized output power vs. superstrate index. System parameters: guide index, 1.47; guide depth, 2 μm; substrate index, 1.46; film thickness, 7 nm; film index, 1.47; gold thickness, 88 nm; gold length, 1.5 mm; $\lambda = 633$ nm.

The final material variable in the sensor structure is the metal film. The choice of a metal for use in a 'bulk' SPR device has been studied before [27]. However, a waveguide SPR sensor for use in the aqueous environment is also partly governed by consideration of the stability and inertness of the metal film to the external environment. If the optical properties of the film change with time then the performance of the sensor will degrade. Gold has been chosen because it is very inert and, with suitable treatment of the glass substrate, can be made extremely adhesive. In addition, gold films provide excellent electrodes for electrochemical studies.

The first design goal was to produce a sensor design that was capable of operating in water and was simple to manufacture, and investigations centred around finding a suitable substrate glass and operating wavelength. During the design process the waveguides were assumed to have a depth of 2 μm and a surface refractive index change of approximately 0.01, compatible with the use of potassium ion exchange. Fig. 4 details the structure and performance of a sensor capable of operating in water at a wavelength of 633 nm. The use of a short wavelength lowers the value of the superstrate

index at which phase matching to a surface plasmon occurs, and Fig. 4 shows that for the given device this occurs at an index of 1.346. The wavelength is also chosen to be compatible with the availability of simple semiconductor sources and the need to operate at a frequency below the plasma frequency of gold to ensure enough damping to create a surface plasmon.

Fig. 4 details the variation in the normalized output power of the sensor as a function of the superstrate index. The figure also shows the change in the normalized output power when a thin layer, of thickness 7 nm and index 1.47, is adsorbed to the surface of the metal film. It is evident that the peak changes in output power occur when the rate of change of the output power with the superstrate index is greatest. This corresponds to a point approximately half way down the dip of the curve of output power against superstrate index in Fig. 4(a). For this design a peak change in normalized output power of 8.1% occurs at a superstrate index of 1.330. Such a change in output power is readily measurable and indicates that the sensor is operable in water. This design has been optimized in terms of the thickness of the gold film and substrate material, but not in terms of the waveguide or the length of the gold film.

In addition to the large sensitivity at a superstrate index of 1.330, Fig. 4(b) shows another region of high sensitivity around a superstrate index of 1.352. A second sensor design employs a dielectric buffer layer to relocate this peak to a superstrate index close to that of water, and increases its magnitude. The structure and performance of this sensor are detailed in Fig. 5. This device generates a maximum change in output power on adsorbing a thin layer of −21.4% at a superstrate index of 1.332. It must be emphasized that this is with respect to the *input* power and that this is achieved against a background transmission of 26.2% in the absence of the thin film. In this instance, the sensor is constructed using a gold film 64 nm thick and a buffer layer of refractive index 1.29 and thickness 328 nm.

Fig. 6 displays the TM mode H_y magnetic field profile for a superstrate index of 1.332, close to that of water, at a wavelength of 633 nm [28]. The mode has a loss of 38.3 dB cm^{-1}, indicating that the useable length of the device would be several millimetres. Considering the two gold/dielectric interfaces in the device, the field intensity is greater at the 'outer' interface between the gold and the superstrate material, illustrating why the design has high sensitivity.

4. Waveguide transmissivity experiments

To validate the waveguide design tool experimentally the output powers of gold-clad potassium ion-exchanged channel waveguides fabricated in soda-lime glass were measured as a function of the length of the

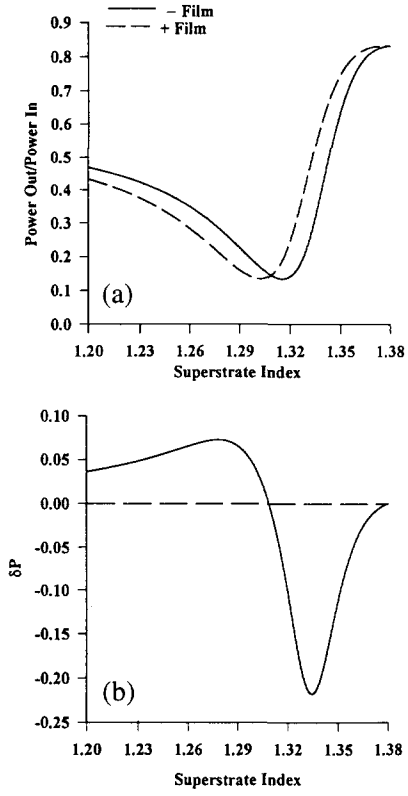

Fig. 5. Performance of a waveguide SPR sensor based on a low refractive index substrate glass, employing a dielectric buffer layer of index 1.29, and operated at a wavelength of 633 nm: (a) normalized output power and (b) change in normalized output power vs. superstrate index. System parameters: guide index, 1.47; guide depth, 2 μm; substrate index, 1.46; film thickness, 7 nm; film index, 1.47; gold thickness, 88 nm; gold length, 1.5 mm; $\lambda = 633$ nm.

gold film. The substrate glass was chosen for the ease of wave-guide fabrication and the low cost of the unprocessed slides. The length of the gold film was varied from 1.5 to 5.4 mm, in 100 μm steps, over a total of 40

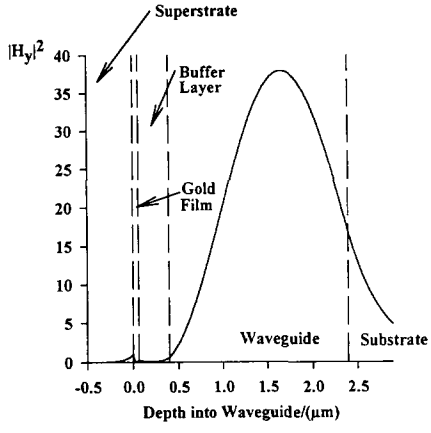

Fig. 6. TM H_y magnetic field plot for the waveguide SPR sensor device detailed in Fig. 5. System parameters: superstrate index, 1.332; gold thickness, 64 nm; buffer index, 1.29; buffer thickness, 328 nm; guide index, 1.47; guide depth, 2 μm; substrate index, 1.46; $\lambda = 633$ nm; loss, 38.3 dB cm^{-1}.

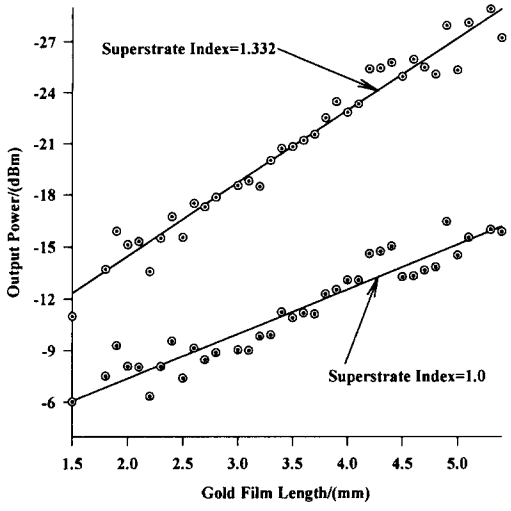

Fig. 7. Variation of the output power of a gold-coated SPR device (plotted in dB m) as a function of the length of the gold film. The curves are labelled with the superstrate index of the device under test. System parameters: gold thickness, 76 nm; guide index, 1.52; guide depth, 2 μm; substrate index, 1.512; $\lambda = 633$ nm.

waveguides, each with a width of 2 μm. The experiment was performed on devices using two superstrate indices, namely, those of air and of water.

Light from a 10 mW linearly polarized He–Ne laser operating at 632.8 nm was passed through a polarizer and end-fire coupled into the waveguide under test. The coupling was then optimized for the waveguide under investigation. The output from the given waveguide was focused onto an optical power meter and readings were taken for each of the 40 waveguides in turn. Air was used as the first superstrate material; subsequently, a silica cell was mounted over the gold film and filled with deionized water. This procedure was sufficient to create a water superstrate over the gold film. The measurements were then repeated on each of the 40 waveguides.

The experiment was carried out for three devices with different thicknesses of gold films, namely, 45, 60 and 76 nm, respectively. The variation in the thickness of each gold film was determined to be $\pm 10\%$ of the quoted thicknesses over the area of each of the gold films.

Logarithmic plots of output power against gold film length were then generated. Least-squares-fit regression lines were fitted to each plot and the slope of the lines and their standard errors determined. In each case, data from damaged or high loss waveguides were ignored. An example plot, including device parameters, is shown in Fig. 7. Each curve is labelled with the device superstrate index. The remaining data are given in Table 1 with theoretical predictions for comparison.

Logarithmic plots of the transmission of the waveguides are linear, as would be expected, and have a high degree of correlation. The TE modal results show the least correlation due to the small change in transmission through the waveguides with gold length. This is because the TE modes will not form a surface plasmon and do not strongly interact with the gold film. Whilst each curve contains the coupling and waveguide losses, these are unimportant as it is the slope of each curve which is compared to the theory. It is clear that the slopes of the curves are greater with water than with air as a superstrate, as predicted. An exact comparison with the theoretical data produced by the waveguide design tool and the experimental data listed here is difficult to make, due to some uncertainty in the modelling data. Specifically the true waveguide parameters, the optical constants of the gold films and the superstrate index are not perfectly known. A systematic error will also be introduced into the theoretical predictions by the use of the step-index slab waveguide approximation of the waveguide design tool. However, in general, the experimental results are in good agreement with theory and are encouraging for future work.

Table 1
Experimental and theoretical rates of change in transmission through gold-coated waveguide SPR devices as a function of the length of the gold film

Gold thickness (nm)	Superstrate index	Mode	Experimental slope (dB mm^{-1})	Theoretical slope (dB mm^{-1})
45	1.000	TE	-0.40 ± 0.08	-0.35
		TM	-2.41 ± 0.08	-2.92
	1.332	TE	-0.42 ± 0.10	-0.36
		TM	-8.75 ± 0.44	-6.54
60	1.000	TM	-2.14 ± 0.08	-2.68
	1.332	TM	-4.07 ± 0.12	-4.68
76	1.000	TM	-2.59 ± 0.14	-2.53
	1.332	TM	-4.25 ± 0.14	-3.31

5. Conclusions

A rigorous waveguide design tool which predicts the behaviour of metal-clad planar waveguide SPR sensors has been established. The model describes the excitation and the propagation of modes in the metal-clad region, resulting in the determination of the device transmission in the presence of sensing films. Two sensor designs for aqueous analytes, operating at around 633 nm, have been generated and similar sensors may be designed for semiconductor sources operating near this wavelength. One design is extremely simple and may be used where optimum sensitivity is not required; the other design incorporates a low-index buffer layer and offers greater sensitivity. Simple planar waveguide SPR devices have been fabricated and tested against the model and agreement with theory is generally good.

Further optimization of these devices, particularly in respect of the waveguide parameters, gold film length and detection system is in progress. It is expected that utilization of this model will lead to the design and realization of waveguide SPR sensors applied to monitoring low concentrations of organic pollutants in water.

Acknowledgements

The authors gratefully acknowledge the support of the EC Environment Programme. The Optoelectronics Research Centre is an Interdisciplinary Research Centre supported by a grant from the UK Science and Engineering Research Council.

References

[1] D. Clerc and W. Lukosz, Integrated optical output grating coupler as refractometer and (bio-)chemical sensor, *Sensors and Actuators B, 11* (1993) 461–465.

[2] J. Ingenhoff, B. Drapp and G. Gauglitz, Biosensor using integrated optical devices, *Fresenius' Z. Anal. Chem., 346* (1993) 580–583.

[3] R. Heidemann, R. Kooyman and J. Greve, Performance of a highly sensitive optical waveguide Mach–Zehnder interferometer immunosensor, *Sensors and Actuators B, 10* (1993) 209–217.

[4] P. Daniels, J. Deacon, M. Eddowes and D. Pedley, Surface plasmon resonance applied to immunosensing, *Sensors and Actuators, 15* (1988) 11–18.

[5] M. Malmqvist, Biospecific interaction analysis using biosensor technology, *Nature, 361* (1993) 186–187.

[6] C.R. Lavers, C. Piraud, M. Brust, K. O'Dwyer, J.S. Wilkinson and D. Schiffrin, Electrochemically-controlled optical waveguide sensors, *Proc. 9th Optical Fiber Sensors Conf. (OFS 9), Firenze, Italy, 4–6 May 1993*, pp. 193–196.

[7] W. Lukosz, Principles and sensitivities of integrated optical and surface plasmon sensors for direct affinity sensing and immunosensing, *Biosensors Bioelectron., 6* (1991) 215–225.

[8] H. Kreuwel, P. Lambeck, J. Beltman and T. Popma, Mode coupling in multilayered structures applied to a chemical sensor and a wavelength selective directional coupler, *Proc. 4th Eur. Conf. Integrated Optics, Glasgow, UK, 11–13 May 1987*, pp. 217–220.

[9] L. Delves and J. Lyeness, A numerical method for locating the zeros of an analytical function, *Math. Comp., 21* (1967) 543–560.

[10] R. Syms and J. Cozens, *Optical Guided Waves and Devices*, McGraw-Hill, London, 1992.

[11] J. Polky and G. Mitchell, Metal-clad planar dielectric waveguide for integrated optics, *J. Opt. Soc. Am., 64* (1974) 274–279.

[12] M. Zervas, Surface plasmon-polariton fiber-optic polarizers using thin-nickel films, *IEEE Photon. Tech. Lett., 2* (1990) 253–256.

[13] P. Kurzynowski, Theoretical analysis of metal-fibre polarizer, *J. Mod. Opt., 40* (1993) 1547–1558.

[14] E. Sharma, M. Singh and P. Kendall, Exact multilayer waveguide design including absorbing or metal layers, *Electron. Lett., 27* (1991) 408–410.

[15] M. Ramadas, E. Garmire, A. Ghatak, K. Thyagarajan and M. Shenoy, Analysis of absorbing and leaky planar waveguides: a novel method, *Opt. Lett., 14* (1989) 376–378.

[16] P. Yeh, *Optical Waves in Layered Media*, Wiley, New York, 1988.

[17] J. Chilwell and I. Hodgkinson, Thin-films field-transfer matrix theory of planar multilayer waveguides and reflection from prism-loaded waveguides, *J. Opt. Soc. Am. A, 1* (1984) 742–753.

[18] A. Ghatak, K. Thyagarajan and M. Shenoy, Numerical analysis of planar optical waveguides using matrix approach, *J. Lightwave Tech., 5* (1987) 660–667.

[19] E. Anemogiannis and E. Glytsis, Multilayer waveguides: efficient numerical analysis of general structures, *J. Lightwave Tech., 10* (1992) 1344–1351.

[20] S. Conte and C. de Boor, *Elementary Numerical Analysis: An Algorithmic Approach*, McGraw-Hill, New York, 2nd edn., 1972.

[21] D. Marcuse, Radiation losses of tapered dielectric slab waveguides, *Bell Syst. Tech. J., 49* (1970) 273–290.

[22] R. Ramaswamy and R. Srivastava, Ion exchanged glass waveguides: a review, *J. Lightwave Tech., 6* (1988) 984–1002.

[23] L. Roß, Integrated optical components in substrate glasses, *Glastech. Ber., 62* (1989) 285–297.

[24] P. Noutsios and Gar Lam Yip, Characterization and modelling of planar surface and buried glass waveguides made by field-assisted K^+ ion exchange, *App. Opt., 31* (1992) 5283–5291.

[25] F. Kou and T. Tamir, Range extension of surface plasmons by dielectric layers, *Opt. Lett., 12* (1987) 367–369.

[26] J. Swalen, R. Santo, M. Tacke and J. Fischer, Properties of polymeric thin films by integrated optical techniques, *IBM J. Res. Dev.*, (Mar.) (1977) 168–175.

[27] H. de Bruijn, R. Kooyman and J. Greve, Choice of metal and wavelength for surface-plasmon resonance sensors: some considerations, *App. Opt., 31* (1992) 440–442.

[28] G. Hale and M. Querry, Optical constants of water in the 200-nm to 200-μm wavelength region, *App. Opt., 12* (1973) 555–563.

Biographies

Richard D. Harris received the B.Sc. degree in applied physics from the University of Bath in 1986. In 1992 he received the M.Sc. degree in applied optics from the University of Salford. He is currently studying for the degree of Ph.D. at the Optoelectronics Research Centre, University of Southampton.

James S. Wilkinson received the B.Sc.(Eng.) in electronics in 1977 and the Ph.D. in the field of integrated optics in 1985, both from University College London. From 1977 to 1979 he was with the GEC Hirst Research Centre working on optical fibre telecommunication systems. From 1983 to 1985 he was with the Department of Nephrology at St. Barth-olomew's Hospital, London, investigating sensing and control techniques for dialysis procedures. He is now senior lecturer in optoelectronics in the Department of Electronics and Computer Science, University of Southampton, partially seconded to the Optoelectronics Research Centre at Southampton University. His research interests include chemical sensors, and integrated optical lasers and amplifiers.